AD-A042 767 MINNESOTA UNIV MINNEAPOLIS DEPT OF AEROSPACE ENGINE--ETC F/G 13/13
STRUCTURAL INELASTICITY XVII. THEORY OF PLASTIC STRUCTURES.(U)
AUG 77 P G HODGE
UNCLASSIFIED AEM-H1-17 N00014-75-C-0177
NL

1 OF 1
AD A042 767

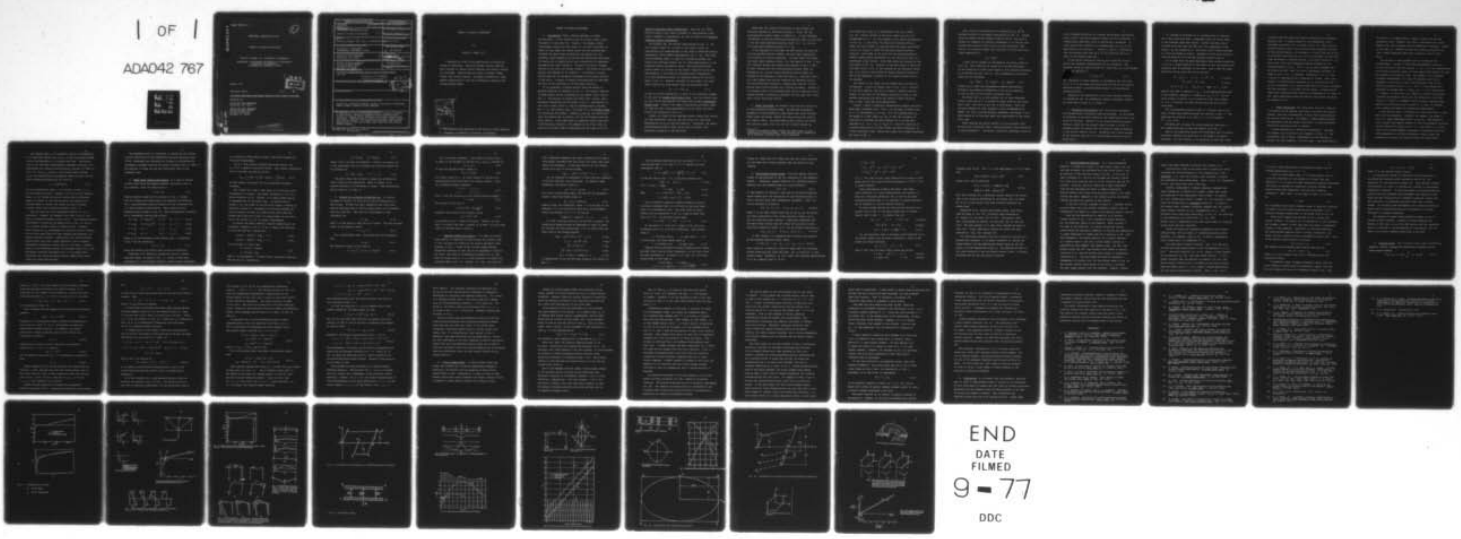

END
DATE FILMED
9-77
DDC

Report AEM-H1-17

STRUCTURAL INELASTICITY XVII

Theory of Plastic Structures

Philip G. Hodge, Jr., Professor of Mechanics

Department of Aerospace Engineering and Mechanics
University of Minnesota
Minneapolis, Minnesota 55455

August, 1977

Technical Report

~~Qualified requesters may obtain copies of this report from DDC~~

Prepared for

OFFICE OF NAVAL RESEARCH
Arlington, VA 22217

OFFICE OF NAVAL RESEARCH
Chicago Branch Office
536 South Clark St.
Chicago, IL 60605

SECURITY CLASSIFICATION OF THIS PAGE (When Data Entered)

REPORT DOCUMENTATION PAGE		READ INSTRUCTIONS BEFORE COMPLETING FORM
1. REPORT NUMBER AEM-H1-17	2. GOVT ACCESSION NO. (9) Technical rept.,	3. RECIPIENT'S CATALOG NUMBER
4. TITLE (and Subtitle) STRUCTURAL INELASTICITY XVII Theory of Plastic Structures	(15) N00014-75-C-0177	5. TYPE OF REPORT & PERIOD COVERED 6. PERFORMING ORG. REPORT NUMBER
7. AUTHOR(s) Philip G. Hodge, Jr., Prof. of Mechanics		8. CONTRACT OR GRANT NUMBER(s) N00014-75-C-0177
9. PERFORMING ORGANIZATION NAME AND ADDRESS University of Minnesota Minneapolis, Minnesota 55455		10. PROGRAM ELEMENT, PROJECT, TASK AREA & WORK UNIT NUMBERS NR 064-429
11. CONTROLLING OFFICE NAME AND ADDRESS OFFICE OF NAVAL RESEARCH Arlington, VA 22217	(11)	12. REPORT DATE August, 1977 13. NUMBER OF PAGES (12) 49p. 46
14. MONITORING AGENCY NAME & ADDRESS (if different from Controlling Office) OFFICE OF NAVAL RESEARCH Chicago Branch Office 536 South Clark St. Chicago, IL 60605		15. SECURITY CLASS. (of this report) Unclassified 15a. DECLASSIFICATION/DOWNGRADING SCHEDULE

16. DISTRIBUTION STATEMENT (of this Report)

Qualified ~~requesters may obtain copies of this report~~ from DDC

DISTRIBUTION STATEMENT A
Approved for public release;
Distribution Unlimited

DDC
AUG 12 1977
RECEIVED
C

17. DISTRIBUTION STATEMENT (of the abstract entered in Block 20, if different from Report)

18. SUPPLEMENTARY NOTES

19. KEY WORDS (Continue on reverse side if necessary and identify by block number)

Plasticity, perfectly-plastic, plastic structures, structures, beams, frames, plates, finite elements

20. ABSTRACT (Continue on reverse side if necessary and identify by block number)

A sampling is given of the applications of plasticity theory to structures. Relations between various theories which include or neglect strain hardening and elastic strains are discussed. Applications are given to trusses, beams, frames, and circular plates. The paper concludes with some general observations on the use of plasticity theories with finite-element models.

DD FORM 1 JAN 73 1473 EDITION OF 1 NOV 65 IS OBSOLETE
S/N 0102-014-6601

SECURITY CLASSIFICATION OF THIS PAGE (When Data Entered)

405 395

THEORY OF PLASTIC STRUCTURES[1]

By

Philip G. Hodge, Jr.[2]

A sampling is given of the applications of plasticity theory to structures. Relations between various theories which include or neglect strain hardening and elastic strains are discussed. Applications are given to trusses, beams, frames, and circular plates. The paper concludes with some general observations on the use of plasticity theories with finite-element models.

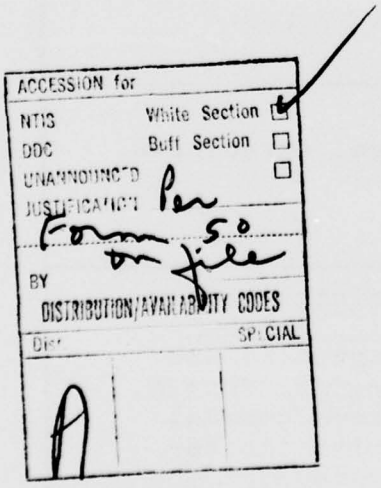

1. This research was sponsored by the Office of Naval Research

2. Professor of Mechanics, University of Minnesota

THEORY OF PLASTIC STRUCTURES

1. Introduction When a tension specimen is loaded monotonically, it will generally have an initial linear range, followed by a nonlinear one. Figure 1, for example, shows experimental results for mild steel [1] and 245-7 aluminum [2]. Figure 1b also shows two fitted curves for the aluminum data. Although the solid curve is certainly the better fit, the piecewise linear dashed curve has obvious theoretical advantages. For simplicity of exposition we shall assume that it adequately represents the "real" material. Points on the first, steeper, portion of the curve are called "elastic", and points on the other portion are referred to as "plastic". A structure is called elastic when all of its parts correspond to the elastic portion of the curve. A theory of plastic structures must be used when any part of the structure is on the plastic portion.

It is convenient to define several idealized models of material behavior as indicated in Fig. 2. The salient features of these models can be illustrated by the simple 3-bar truss in Fig. 3. The results of loading the truss with a slowly, monotonically increasing load are shown in Fig. 4. The behavior of the "real" truss, curve (a), may be characterized as follows. For $P < P_A$, the elastic limit, the truss is in the elastic range—all three bars are elastic. Between P_A and P_B, the yield-point load, the central bar is plastic, but the two diagonal bars are still elastic. Since these bars by themselves would constitute a load-carrying structure, the response of the 3-bar truss is still of an elastic order of magnitude and the truss is in the

range of contained plastic deformation. Along BC, all three bars are plastic and a small increment of load produces a much larger increment of deformation, so that we refer to the range of extensive plastic deformation.

We consider now, the various idealizations of Fig. 3. The fully elastic model (b) is exact in the elastic range, an increasingly poor approximation in the range of contained plastic deformation, and an absurd approximation for $P > P_B$. The rigid/strain-hardening model (c) does not distinguish between the elastic and contained ranges, but is a good approximation to the extensive plastic deformation range. The elastic/perfectly-plastic model (d) is exact in the elastic range and a very good approximation in the range of contained plastic deformation. It is also essentially exact for moderate strains for the mild steel of Fig. 1a. However, according to this model, the truss cannot support any load greater than the yield-point load

$$P_0 = (1 + \sqrt{2})A\,\sigma_0 \qquad (1.1)$$

so that it is more appropriate to refer to the horizontal segment of the curve as unrestricted plastic flow. Any load greater than P_0 could not be equilibrated and hence would produce accelerated plastic flow. Finally, the simple rigid/perfectly-plastic model (a) does not give a good approximation in any range, but does predict the yield-point load (1.1).

Indeed, all three of the idealized plastic models have exactly the same yield-point load P_0, and this value is a very good approximation to P_B for the real material. Therefore, the simple rigid/perfectly-plastic model can be used to predict this significant property of the structure.

Based upon this simple illustration, we may propose the following approach to structural analysis. First, use the rigid/perfectly-plastic model to predict P_0. If more detailed information is required concerning deformations under a given load P, use the elastic/perfectly-plastic model if $P < P_0$, and use the rigid/strain-hardening model if $P > P_0$.

In the remainder of this paper we shall mostly be concerned with the perfectly-plastic models, and with their application to structures of various complexity. We shall begin with beams and frames under bending in Secs. 2-4, add tension in Sec. 5, and then consider torsion and torsion with tension in Secs. 6 and 7. We shall discuss both the rigid/perfectly-plastic mdoel for determining P_0, and the elastic/perfectly-plastic model for discussing the response at loads less than P_0. Sections 8 and 9 will then present more general theories for perfectly-plastic and strain-hardening materials, respectively, and Sec. 10 will analyze some circular plates for a variety of models. Section 11 will present some of the problems which exist in applying finite element methods to plasticity problems, and the paper will close with a brief concluding section.

2. Beams and Frames. We consider first the pure bending of an elastic/perfectly-plastic beam. We make the fundamental assumption of Euler-Bernouilli beam theory that plane sections remain plane and normal, whence the strain across the section will remain linear. For sufficiently small strains the stress will also be linear, Fig.* 5a, but for a certain moment M_e

*Figure 5 and several other figures are taken from [3] with permission of the publisher. Such figures will be identified by an asterisk following their first reference.

the stress will reach σ_0 in magnitude at the outer fibers, Fig. 5b. Greater strains in the outer fibers can still be accomodated by $|\sigma| = \sigma_0$, thus leading to the stress distribution in Fig. 5c. In the limit, the strain will become infinite under the finite moment M_0 obtained from the stress distributon in Fig. 5d. Figure* 6 shows the resulting moment-curvature relation. Curve OABD is the curve for the elastic/perfectly-plastic section being considered, for the particular case of a rectangular cross section. Curve OABC shows the diagram for the mild steel of Fig. 1a. However, in the same spirit in which the nonlinear curve in Fig. 1b was replaced by the piecewise linear one, it is usual to solve beam and frame problems according to OED or OFD depending on whether or not elastic strains are to be included.

The effect of the "knee" AB will depend upon the shape of the section. It will be greater than in Fig. 6 for a circular or cruciform section, less for an I-beam or sandwich section. Indeed, in the limit as the bending resistance of web or core becomes negligible even while the flange or sheet thickness goes to zero, curve OED would become exact.

Figure* 7 shows a statically indeterminate propped cantilever beam under increasing load. For $F \leq F_1$ the beam is elastic and at $F = F_1$ the moment at A is $-M_0$. As F is increased above F_1, the moment at A must remain at $-M_0$, so that the increment of load above F_1 produces the same response as if a hinge were inserted at A. At $F = F_0$, $M = M_0$ at B. Since the insertion of a second yield-hinge at B would render the beam a mechanism, F_0 is the yield-point load. Notice how closely this example parallels the truss in Sec. 1.

Now, if we are interested only in predicting F_0, we may proceed directly to the moment distribution of Fig. 7e. Indeed, since the moment varies linearly along AB and BC, and since 2 hinges are necessary to produce a mechanism, it is obvious that we must have hinges at both A and B at the yield-point load. Statics, or even more simply the Principle of Virtual Work, then leads immediately to

$$F_0 = 3M_0/L \tag{2.1}$$

A less trivial example is furnished by the portal frame in Fig.* 8a. This frame can be turned into various mechanisms by the insertion of three yield hinges in four possible locations as illustrated by Figs. 8b,c,d. The corresponding yield-point loads are all different:

$$F_b = 2M_0/L \qquad F_c = M_0/2L \qquad F_d = 5M_0/8L \tag{2.2}$$

Figures 8e,f,g show the corresponding moment distributions. Evidently the moments corresponding to F_b and F_d exceed M_0, so that F_c must be the correct yield-point load.

We notice that F_c is the smallest of the three mechanism loads so that any of (2.2) provide an upper bound on the yield-point load. This fact is not just a coincidence. There are two basic theorems of limit analysis, proved independently by Gzodev [4], Hill [5,6], and Drucker, Greenberg, and Prager [7,8,9] which enable us to find both upper and lower bounds on the yield-point load.

These theorems are easily stated in a quite general form. We are given a structure with a load distribution fully defined by a single parameter P. We define a statically admissible field as

a set of moments which are in internal and external equilibrium with a load P^- and which nowhere violate the yield condition. A kinematically admissible field is defined by a mechanism. At every yield hinge a moment M is assigned equal to $\pm M_0$ in the same sense as the rotation θ. Finally a load P^+ is defined so that the external work done by P^+ on the mechanism motion is equal to the internal work $\Sigma M\theta$.

At the actual yield-point load P_0 all conditions of both static and kinematic admissibility will be satisfied. The theorems, which are easily proved [3], state that P_0 is the largest P^- and the smallest P^+:

$$P^- \leq P_0 \leq P^+ \qquad (2.3)$$

The importance of these theorems is increased by the fact that P_0 in (2.3) is the same yield-point load for any of the elastic/perfectly-plastic, rigid/perfectly-plastic, or rigid/strain-hardening models.

Examples of the application of the limit analysis theorems to rectangular and non-rectangular frames, Vierendeel trusses, and grids may be found in [3, Chap. 3].

3. Unloading and reloading. Thus far we have considered only monotonically increasing loads and stresses. If the stress is decreased in an elastic material, the stress-strain curve will simply be retraced. However, for an elastic/perfectly-plastic material loaded into the plastic range to point B in Fig. 9, unloading would not retrace BAO, but would be along BC parallel to the initial elastic line OA. Reloading from C would retrace CD and continue along BD as if the unloading excursion had not taken place.

If, instead of reloading at C, unloading were to continue until the stress were zero, a permanent strain OE would remain in the speciman under zero stress. Further unloading would continue along the same line BCE until the compressive yield stress, $-\sigma_0$ was reached at F. The strain could further decrease to G with no change in stress. Reloading at this point would be along GH parallel to BF and the original elastic line OA.

It is clear from the above description that neither stress nor strain is a unique function of the other, so that the constitutive relations must be expressed in rate form. With a need for later generality we may write the law as follows:

$$\sigma^2 - \sigma_0^2 \leq 0 \qquad \dot{\lambda} \geq 0 \qquad \dot{\varepsilon} = \dot{\varepsilon}^e + \dot{\varepsilon}^p \qquad (3.1a,b,c)$$

$$\dot{\varepsilon}^e = E^{-1}\dot{\sigma} \qquad \dot{\varepsilon}^p = 2\dot{\lambda}\sigma \qquad (3.1d,e)$$

$$\text{IF } \sigma^2 - \sigma_0^2 < 0 \quad \text{OR } 2\sigma\dot{\sigma} < 0 \quad \text{THEN } \dot{\lambda} = 0 \qquad (3.1f)$$

Observe that when σ remains at $+\sigma_0$, $\dot{\varepsilon}$ is not determined but must be non-negative, whereas if σ remains at $-\sigma_0$, $\dot{\varepsilon} \leq 0$. For any given history of strain it will always be clear which branch of (3.1) is relevant, so that the equations may be trivially integrated.

The rigid/perfectly-plastic model is a special case of the above in which the elastic portions are vertical in Fig. 9. The equations are given by (3.1) with $E = \infty$ in (3.1d), whence $\dot{\varepsilon}^e = 0$ in (3.1c).

Unloading and reloading for strain-hardening materials is more complicated and we delay the subject until Sec. 9.

Some of the simplified results and techniques used in plastic structural analysis are valid only in the absence of plastic unloading. For this reason, it is important to note that local

unloading may take place even under a monotonically increasing external load. A simple example of this phenomenon, first discussed by Drucker [10], is shown in Fig. 10. Three elastic/perfectly-plastic bars, with relative yield strengths indicated by the circled numbers, are attached to a fixed rigid bar AB and an otherwise free rigid bar CD. As P is increased, all bars will first be elastic in tension and bar 1 will yield first at $P = P_1$. Bars 2 and 3 will have increasing tensile stresses as P is increased above P_1 to P_2. For $P > P_2$ the load increment must be carried by bars 1 and 2 so that a compressive increment is added to bar 1, i.e., it unloads. Eventually, at $P = P_0$, bar 1 yields in compression and a mechanism is formed. Thus, even though P is monotonically increased to P_0, the stress in bar 1 is first increased to σ_0, remains there while its strain increases, and then decreases to $-\sigma_0$ when failure occurs. A simple portal frame which exhibits similar behavior is discussed in [3, Chap. 4], and a more complicated truss with several such stress reversals is analyzed in [11].

4. Other limitations. The yield-point load will always be a limitation on the maximum load which a structure can support. However, there are circumstances in which other considerations may be more restrictive. For example, slender members subject to compressive load may buckle elastically or even plastically before the yield-point load is reached.

Another possibility is excessive deformations. Consider, for example [12] the beam on four supports in Fig.* 11. The yield-point load is $4M_0/L$, independently of the distance ζL between the outer supports. For very small ζ the configuration

is similar to a clamped beam of length 2L which has the same yield-point load. However, for large ζ the effective strength added by the outer supports would be expected to decrease. Indeed, in the limit as ζ becomes infinite the central span should act like a simply supported beam whose yield-point load is only $2M_0/L$.

The solution of this paradox lies in considering the displacements. Figure* 12 shows the displacements just prior to the yield-point load for various ζ. For $\zeta = 10$ the displacements would almost certainly render the beam unservicable before the load has reached its yield-point load. For example, if the maximum allowable displacement is 5 times the maximum elastic displacement in the built-in beam, the yield-point load is the limiting criterion only if $\zeta \leq 2$. For $\zeta = 5$ the maximum displacement is reached when $F = 3M_0/L$, for $\zeta = 10$ it occurs when $F = 2.5M_0/L$. In the limit, as ζ tends to infinity, the maximum allowable displacement occurs with the formation of the first hinge at $F = 2M_0/L$ in agreement with the simply supported beam. Details of the solution may be found in [3, Chap. 4] together with a simplified method for estimating displacements.

A less obvious type of limitation can occur when there is more than one load parameter. Consider, for example, the frame in Fig.* 13, under independent loads F_1 and F_2. The methods of limit analysis are readily adapted to this two-parameter situation, and the results are shown in Fig.* 14. Load points $f_i = LF_i/M_o$ lying on the hexagon MNPQRS correspond to yield-point with each side representing a different mechanism, points inside the hexagon do not yield, and points outside are unattainable.

Now suppose that f_2 is increased to point A corresponding to a fixed dead weight load, and f_1 is then alternated between A and B corresponding to a variable wind load. The plastic part of the resultant displacements, computed according to an approximate but complete elastic-plastic analysis, is shown in Fig.* 15. Here δ_{1p} refers to the dimensionless sidesway, δ_{2p} to the dimensionless displacement under the load, and the actual dimensioned quantities are given by

$$\Delta_i = (M_0 L^2/6EI)\delta_i \qquad (4.1)$$

For the rigid/plastic model, E is infinite so that $\Delta_i = 0$ for any number of cycles. However, for any finite E, however large, Δ_i will become arbitrarily large after a sufficient number of cycles, so that the structure can support only a limited number of cycles even though the load is always strictly within the yield-point hexagon of Fig. 14.

Even one load can cause undesirable behavior if it is alternated. Suppose, for example, that there is no f_1, but that f_2 alternates between points A and C. The resulting plastic displacement is shown by the dashed curve in Fig. 15, and is not in itself alarming since it remains finite. However, each increase in δ_{1p} corresponds to a positive plastic rotation of the yield hinge under the load, whereas each decrease is a negative plastic rotation. Construction of a moment-rotation diagram would show that a large hysterisis loop is present, representing substantial energy input to the hinge. Although details of the phenomenon cannot be discussed within any of the macroscopic theories considered here, it is evident that a relatively few cycles may cause internal damage which would render the frame unserviceable.

The shakedown load of a structure is defined as the largest load for which none of the undesirable features described above occurs. Techniques are available for finding or estimating the incremental collapse load and the cyclic collapse load [3, Chap. 5]. The smallest of these two and the yield-point load is the shakedown load.

5. Beams under tension and bending. If a beam is subject to both axial force and bending moments, the strain rate at any distance z from the center axis is

$$\dot{\varepsilon} = \dot{e} + z\dot{\kappa} \tag{5.1}$$

Elastic-plastic stages will be similar to Fig. 5, except that the neutral and center axes will generally be different. For a rigid/perfectly-plastic material we are interested only in a fully plastic cross section. Here, there are four possibilities as shown in Fig. 16. The corresponding resultants for a rectangular section must satisfy

$$N = -N_0\zeta \quad M = M_0(1-\zeta^2) \quad \dot{\kappa} \geq 0 \quad -1 < \zeta < 1 \tag{5.2a}$$

$$N = N_0\zeta \quad M = -M_0(1-\zeta^2) \quad \dot{\kappa} \leq 0 \quad -1 < \zeta < 1 \tag{5.2b}$$

$$N = -N_0 \quad M = 0 \quad \dot{e} \leq 0 \quad |\zeta| \geq 1 \tag{5.2c}$$

$$N = N_0 \quad M = 0 \quad \dot{e} \geq 0 \quad |\zeta| \geq 1 \tag{5.2d}$$

where ζh is the distance to the neutral axis. In addition, $\dot{e}$ and $\dot{\kappa}$ must be related by

$$\dot{e} + \zeta\,\dot{\kappa} = 0 \tag{5.3}$$

since the neutral axis strain rate is zero by definition.

Equations (5.2) define an interaction curve in stress-resultant space, as shown in Fig. 17. Points on the curve correspond to a fully-plastic section, points within correspond

to a section at least partly elastic, and points outside the curve are unobtainable.

Let $\underset{\sim}{Q} = (N,M)$ denote a generalized stress vector, and $\underset{\sim}{q} = (\dot{e},\dot{\kappa})$ a general strain-rate vector. The internal dissipation rate of the beam can then be written

$$D_{int} = \int_V \sigma\dot{\varepsilon}dv = \int_0^L (N\dot{e} + M\dot{\kappa})dx = \int_0^L \underset{\sim}{Q}\cdot\dot{\underset{\sim}{q}}\, dx \qquad (5.4)$$

so that Prager's criterion [13] for genralized variables satisfied.

Now, except for A and D, each point $\underset{\sim}{Q}$ on the yield curve corresponds to a unique ζ and hence, according to (5.3) to a unique direction for $\dot{\underset{\sim}{q}}$. Further, it is easily shown that $\dot{\underset{\sim}{q}}$ is perpendicular to the yield curve. At points A and D neither ζ nor the normal to the curve are unique. However all admissible values of ζ correspond to directions between the limiting normals so that in a sense we may state that the generalized strain-rate vector is always normal to the yield curve. The length of $\dot{\underset{\sim}{q}}$ is, of course, undetermined.

To express the above geometric results algebraically, we eliminate ζ between (6.2a) or (6.2b) to obtain the equations for arcs DBA and DEA, respectively:

$$f_1(N,M) \equiv (N/N_0)^2 + M/M_0 - 1 = 0 \qquad (5.5a)$$

$$f_2(N,M) \equiv (N/N_0)^2 - M/M_0 - 1 = 0 \qquad (5.5b)$$

If $\dot{\underset{\sim}{q}}$ is normal to (5.5a) then

$$\dot{e} = \dot{\lambda}\partial f/\partial N = 2\dot{\lambda}N/N_0^2$$
$$\dot{\kappa} = \dot{\lambda}\partial f/\partial M = \dot{\lambda}/M_0 \qquad (5.6)$$

where $\dot{\lambda}$ is non-negative. In vector form, the strain rates for DBA and DEA are, respectively

$$\dot{\underset{\sim}{q}} = \dot{\lambda}\underset{\sim}{\nabla}f_1(\underset{\sim}{Q}) \qquad \dot{\underset{\sim}{q}} = \dot{\mu}\underset{\sim}{\nabla}f_2(\underset{\sim}{Q}) \tag{5.7}$$

where $\dot{\lambda}$ and $\dot{\mu}$ are each non-negative. Finally, at points D or A the requirement that $\underset{\sim}{q}$ lie between the limiting normals can be expressed by

$$\dot{\underset{\sim}{q}} = \dot{\lambda}\underset{\sim}{\nabla}f_1 + \dot{\mu}\underset{\sim}{\nabla}f_2 \qquad \dot{\lambda} \geq 0 \quad \dot{\mu} \geq 0 \tag{5.8}$$

The above theory may be used to assess the influence of axial forces on the yield-point loads of frames, or to analyze problems of curved beams or arches. Some applications may be found in [3, Chap. 7].

6. Torsion of a circular cylindrical bar. A circular cylinder of length L is fixed at one end and subjected to a pure torque. We make the usual assumption that each cross section undergoes only a rotation proportional to its distance from the fixed end. Then the only displacement is the tangential one

$$v = \alpha z r \tag{6.1}$$

where α is the angle of twist per unit length. The only non-zero strain is the shearing strain

$$\gamma = \gamma_{\theta z} = \alpha r \tag{6.2}$$

For α sufficiently small, the entire bar will be elastic with

$$\tau = G\alpha r \tag{6.3}$$

The resultant torque in this case is

$$T = 2\pi \int_0^a r\tau r \, dr = (\pi/2)G\alpha a^4 \tag{6.4}$$

As α is slowly increased, τ will reach its yield value k in shear at the boundary of the bar for a value α_1 defined by

$$G\,\alpha_1\,a = k \tag{6.5}$$

so that the maximum elastic torque is

$$T_1 = (\pi/2)ka^3 \tag{6.6}$$

For larger values of α , an outer annulus of the bar will become plastic while the inner core remains elastic. Thus, for a perfectly-plastic material

$$\begin{aligned} \tau &= G\alpha r \qquad 0 \leq r \leq \rho \\ \tau &= k \qquad\quad \rho \leq r \leq a \end{aligned} \tag{6.7}$$

Since τ must be continuous at the elastic-plastic boundary ρ,

$$\rho = k/G\alpha \tag{6.8}$$

The torque in this case is

$$T = \frac{2}{3}\,\pi k a^3 [1 - \frac{1}{4}\,(\frac{k}{G\alpha a})^3] \tag{6.9}$$

Evidently the limiting fully plastic torque

$$T_0 = (2/3)\,\pi k a^3 \tag{6.10}$$

is attained only as α tends to infinity. However, we note that T is within less than 1 percent of T_0 when α is only three times its maximum elastic value α_1.

7. Combined tension and torsion. If a beam of circular cross section is subjected to both tension and torsion, then it will certainly be limited by the tensile and shear yield stresses σ_0 and k. These values are both experimentally determined constants so that one can be expressed in terms of the other, and there is considerable evidence that $\sigma_0 = \sqrt{3}k$. Thus the stress point $\underset{\sim}{Q} = (\sigma,\tau)$ must certainly lie within the rectangle ABCD in Fig. 18. However, if σ and τ are both non-

zero, experience suggests that their interaction will pose a more severe limitation and that $\underset{\sim}{Q}$ must lie within some curve within the rectangle. In the next section we will justify taking this curve to be the ellipse

$$f(\underset{\sim}{Q}) \equiv [\sigma^2/3 + \tau^2]/k^2 - 1 = 0 \qquad (7.1)$$

Let us visualize an experiment in which the unit extension e and unit rotation α are controlled. In terms of these parameters, the strain vector is

$$\underset{\sim}{q} \equiv (\varepsilon,\gamma) = (e,\alpha r) \qquad (7.2)$$

For e and α sufficiently small, the bar will be everywhere elastic, hence the stress vector is

$$\underset{\sim}{Q} \equiv (\sigma,\tau) = G(3e,\alpha r) \qquad (7.3)$$

where we have, for simplicity, taken $\nu = 1/2$ so that $E = 3G$. Equation (7.3) will be valid so long as $\underset{\sim}{Q}$ lies everywhere within the ellipse (7.1), i.e., so long as

$$(\sqrt{3}Ge/k)^2 + (G\alpha a/k)^2 - 1 \leq 0 \qquad (7.4)$$

If e and α are such that part of the bar is plastic, the constitutive equations must be expressed in terms of rates. To this end, we first rewrite Eqs. (3.1) in vector form and apply them to the present problem:

$$f(\underset{\sim}{Q}) \equiv (1/k^2)(\sigma^2/3 + \tau^2) - 1 \leq 0 \qquad (7.5a)$$

$$\dot{\lambda} \geq 0 \qquad \dot{\underset{\sim}{q}} = \dot{\underset{\sim}{q}}^e + \dot{\underset{\sim}{q}}^p \qquad (7.5b,c)$$

$$\dot{\underset{\sim}{q}}^e = G^{-1}(\dot{\sigma}/3,\dot{\tau}) \qquad (7.5d)$$

$$\dot{\underset{\sim}{q}}^p = \dot{\lambda}\underset{\sim}{\nabla} f = 2(\dot{\lambda}/k^2)(\sigma/3,\tau) \qquad (7.5e)$$

$$\text{IF } f < 0 \text{ OR } f < 0 \text{ THEN } \dot{\lambda} = 0 \qquad (7.5f)$$

In generalizing (3.1e) we have been guided by the results of Sec. 5.

Let us consider specifically the case where $\dot{\lambda} > 0$. It then follows from (7.5f) that $f = \dot{f} = 0$, whence the local dissipation rate is

$$\underset{\sim}{Q} \cdot \dot{\underset{\sim}{q}} = \frac{1}{G}\left(\frac{\sigma\dot{\sigma}}{3} + \tau\dot{\tau}\right) + \frac{2\dot{\lambda}}{k^2}\left(\frac{\sigma^2}{3} + \tau^2\right) = 2\dot{\lambda} \qquad (7.6)$$

We can now rewrite Eqs. (7.5) in the more useable form

$$f(\underset{\sim}{Q}) \leq 0 \qquad Q\cdot\dot{q} \geq 0 \qquad (7.7a,b)$$

IF $f < 0$ OR $\dot{f} < 0$ THEN

$$\dot{\sigma} = 3G\dot{e} \qquad \dot{\tau} = Gr\dot{\alpha} \qquad (7.7c)$$

ELSE

$$\dot{\sigma} = (G/k^2)[3k^2 - \sigma^2)\dot{e} - \sigma\tau r\dot{\alpha}]$$
$$\dot{\tau} = (G/k^2)[-\sigma\tau\dot{e} + (k^2 - \tau^2)r\dot{\alpha}] \qquad (7.7d)$$

Let us consider a specific loading sequence in which e is slowly increased from 0 to $k/\sqrt{3}G$ and is then held there while α is increased to k/Ga. The first stage is fully elastic and is governed by (7.7c) or, since we start from zero, by (7.3). At the end of this stage

$$e = k/\sqrt{3}G \qquad \sigma = k\sqrt{3} \qquad \alpha = \tau = 0 \qquad (7.8)$$

At this point $f = 0$ for all r, hence (7.7d) are to be integrated with (7.8) as initial conditions. This process leads to

$$\sigma = k\sqrt{3}\ \text{sech}\ (G\alpha r/k) \qquad \tau = k\ \tanh\ (G\alpha r/k) \qquad (7.9)$$

In particular, the final stress state is

$$\sigma = k\sqrt{3}\ \text{sech}\ (r/a) \qquad \tau = k\ \tanh\ (r/a) \qquad (7.10)$$

Consider now an alternative loading sequence which reaches the same final state by first increasing α to its final value, and then increasing e. As shown in [14, Sec. 14], the final stress state in this case is

$$\sigma = k\sqrt{3}\ \tanh\ \xi \qquad \tau = k\ \text{sech}\ \xi$$
$$\xi = 1 - u + \tanh^{-1} u \qquad u = \sqrt{1 - r^2/a^2} \qquad (7.11)$$

Figure 19, taken from [14] shows how much the stress solution for the same final strains depends upon the history of the loading.

8. Multi-axial stress states. The most general state of stress is characterized by the six components of the symmetric tensor $\underset{\sim}{\sigma}$. Therefore, general behavior of a perfectly-plastic material will be characterized by a yield condition

$$f(\underset{\sim}{\sigma}) \leq 0 \tag{8.1}$$

If the material is isotropic, the form of the yield condition cannot depend upon the orientation of the coordinate axes, so that f can have only three independent arguments. Thus (8.1) can be replaced by either of

$$f(\bar{\sigma}, J_2, J_3) \leq 0 \qquad f(\sigma_1, \sigma_2, \sigma_3) \leq 0 \tag{8.2a,b}$$

where $\bar{\sigma}$ is the mean normal stress and J_2 and J_3 are the second and third invariants of the stress deviation tensor, and σ_i are the three principal stresses. Experience indicates that the mean normal stress does not affect the yielding of most structural materials whence (8.2) can be further simplified to

$$f(J_2, J_3) \leq 0 \qquad f(\sigma_1-\sigma_3, \sigma_2-\sigma_3) \leq 0 \tag{8.3a,b}$$

In 1868, Tresca [15] suggested that yielding was governed by the maximum shearing stress, hence

$$f = \max [|\sigma_1 - \sigma_2|, |\sigma_1 - \sigma_3|, |\sigma_2 - \sigma_3|] - 2k \tag{8.4}$$

This condition is generally simple to apply when the principal stress directions are fixed and known but is difficult in more general cases. Therefore, in 1913, Mises [16] proposed approximating (8.4) by a special case of (8.3a):

$$f = 6J_2 - 2\sigma_0^2$$
$$= (\sigma_x - \sigma_y)^2 + (\sigma_x - \sigma_z)^2 + (\sigma_y - \sigma_z)^2$$
$$+ 6(\tau_{xy}^2 + \tau_{xz}^2 + \tau_{yz}^2) - 2\sigma_0^2 \qquad (8.5)$$

If $\sigma_0 = \sqrt{3}k$, then the two yield conditions will agree in pure shear and will have their maximum discrepancy of $2/\sqrt{3} = 1.155$ in simple tension.

Later experimental evidence has shown, that Mises' yield condition is a closer approximation than Tresca's to most real structural materials, but in view of the small difference between them, it is customary to assume whichever one is simplest in a given problem situation.

We have already derived the constitutive equations for a special case in Sec. 5, and have assumed them in another special case in Sec. 7. In general they are

$$f(\underset{\sim}{\sigma}) \leq 0 \qquad \dot{\lambda} \geq 0 \qquad \dot{\underset{\sim}{\varepsilon}} = \dot{\underset{\sim}{\varepsilon}}^e + \dot{\underset{\sim}{\varepsilon}}^p \qquad (8.6a,b,c)$$

$$\dot{\underset{\sim}{\varepsilon}}^e = \underset{\sim}{E}^{-1}\dot{\underset{\sim}{\sigma}} \qquad \dot{\underset{\sim}{\varepsilon}}^p = \dot{\lambda}\nabla f \qquad (8.6d,e)$$

$$\text{IF } f < 0 \text{ OR } \dot{f} < 0 \text{ THEN } \dot{\lambda} = 0 \qquad (8.6f)$$

For the particular case of the Mises yield condition (8.5), the general results may be simply expressed in terms of the stress and strain deviators

$$\underset{\sim}{s} = \underset{\sim}{\sigma} - \underset{\sim}{I}\bar{\sigma} \qquad \underset{\sim}{e} = \underset{\sim}{\varepsilon} - \underset{\sim}{I}\bar{\varepsilon} \qquad (8.7)$$

where $\bar{\sigma}$ and $\bar{\varepsilon}$ are the mean normal stress and strain:

$$f \equiv \underset{\sim}{s}:\underset{\sim}{s} - 2k^2 \leq 0 \qquad \dot{\lambda} \geq 0 \qquad (8.8a,b)$$

$$\dot{\underset{\sim}{e}} = \dot{\underset{\sim}{s}}/2G + \dot{\lambda}\underset{\sim}{s} \qquad \bar{\sigma} = 3K\bar{\varepsilon} \qquad (8.8c,d)$$

together with (8.6f). For $\dot{\lambda} > 0$, the requirement $f = \dot{f} = 0$ shows that

$$\underset{\sim}{\dot{e}}:\underset{\sim}{s} = \underset{\sim}{\dot{s}}:\underset{\sim}{s}/2G + \dot{\lambda}\underset{\sim}{s}:\underset{\sim}{s} = 2k^2\dot{\lambda} \tag{8.9}$$

whence (8.8) can be rewritten

$$\begin{aligned} &\text{IF } f < 0 \text{ OR } \dot{f} < 0 \text{ THEN } \underset{\sim}{\dot{s}} = 2G\underset{\sim}{\dot{e}} \\ &\text{ELSE } \underset{\sim}{\dot{s}} = 2G[\underset{\sim}{\dot{e}} - \underset{\sim}{s}(\underset{\sim}{\dot{e}}:\underset{\sim}{s})/2k^2 \end{aligned} \tag{8.10}$$

Note that although for a perfectly plastic material the strain rate is not uniquely determined by the stress rate, as shown by (8.10) a given strain rate does uniquely determine the stress rate.

Equations (8.8), without the elastic terms, were first used by Mises in 1913 [16], following ideas advanced by St. Venant [17] and Levy [18] in 1870. The elastic terms were incorporated by Prandtl [19] and Reus [20] in 1924 and 1930. The more general (8.6) were first proposed by Mises in 1928 [21]. Later, additional reasons for using them were advanced by Hill [22], Drucker [23].

For structural problems which are coveniently handled with generalized variables, it is merely necessary to replace the stress matrix $\underset{\sim}{\sigma}$ by the generalized stress vector $\underset{\sim}{Q}$, and the strain $\underset{\sim}{\varepsilon}$ by the generalized strain $\underset{\sim}{q}$. The appropriate form of the yield condition f and the elastic matrix $\underset{\sim}{E}$ must, of course, be determined for the particular structure.

9. Strain-hardening material. If a strain-hardening material is loaded to a point B in the plastic range, Fig. 20, and then unloaded, the unloading will take place along a line BC parallel to the original elastic line OA. If the load is again reversed at C, CB will be retraced and further loading will take place along BD just as if the excursion BCB had not occured. Actually, BCB will constitute a small hysteresis loop and the reloading may start to behave plastically shortly before B and rejoin line AD shortly after B, but these effects are small compared to the overall elastic and plastic effects and hence are ignored in most models.

If the bar is fully unloaded to point E, a residual strain OE will remain and, with further unloading, plastic flow in compression will begin at a point F and continue along a line FG.

Thus far the description of behavior is an obvious generalization of Fig. 9 for a perfectly-plastic material, but two questions remain to be answered: where is point F and what is the slope FG? If elastic slopes and initial yield-stress are originally symmetric in tension and compression, it seems reasonable to assume that FG is parallel to AB. With this assumption, the future behavior of a tensile speciman at a generic point C and with a given loading history is specified by four numbers: the elastic slope (OA, FB), the plastic slope (AB, GF), the current yield stress in tension (ordinate of B), and the current yield stress in compression (ordinate of F). The two slopes are material constants independent of history, and, for the history shown in Fig. 20, the current tensile yield stress is the value σ_1 at which the most recent plastic flow was reversed. However, various

models have been proposed to predict the ordinate of F.

Historically, most of the early work in plasticity which accounted for strain-hardening at all assumed that it was isotropic, i.e., that the current yield stresses in tension and compression were always equal. Thus, in Fig. 20, compressive plastic flow would take place along F_3G_3.

However, experimental evidence generally suggests that strain hardening in tension will reduce, rather than raise, the magnitude of the compressive yield stress. To account for this "Bauschinger effect," Prager [24, 25] proposed a theory which has become known as kinematic hardening. In terms of the tension test, kinematic hardening assumes that the elastic range remains constant at $2\sigma_0$, independently of σ_1. Thus unloading would take place along BF_1G_1 in Fig. 20. We note that if the hardening is so great that $\sigma_1 > 2\sigma_0$, then plastic flow in compression would take place under an unloading stress which was still positive.

These two models are generally accepted as the extreme possibilities, and any number of intermediate models can be proposed. For example, F_2G_2 in Fig. 20 shows a compressive yield stress which is independent of σ_1.

For multi-axial status of stress, Eqs. (8.6) may still be used with some modifications in the interpretation of $f(\underset{\sim}{\sigma})$ and $\dot{\lambda}$. The yield function $f(\underset{\sim}{\sigma})$ is no longer a fixed property of the material but will vary with stress history. It will remain constant when the behavior is elastic, but will vary during plastic flow so that $\underset{\sim}{\sigma}$ is always on the yield surface. Thus one should write $f = f(\underset{\sim}{\sigma}, H)$ where H stands symbolically for the entire stress-strain history. Then, in Eq. (8.6f),

$\dot{f}$ is not a total derivative of the entire function, but is defined specifically by $\dot{f} = \nabla f \cdot \dot{\sigma}$.

Since the requirement that f = 0 during plastic flow is a partial constraint on the history of f rather than the equation $\dot{f} = 0$, we have one fewer constitutive equation available. The system is balanced by requiring a relation between the plastic strain-rate magnitude $\dot{\lambda}$ and the yield function increase $\dot{f}$. Thus, when $\dot{\lambda}$ is not equal to zero, it is given by

$$\dot{\lambda} = B\dot{f} \tag{9.1}$$

For a hardening curve with variable slope, B could be a function of stress; for the linear hardening here considered, B is a material constant proportional to the slope of AB in Fig. 20.

There still remains the problem of how f varies with plastic loading. One reason for the popularity of the isotropic and kinematic models is that they both give easily implemented answers to that question. According to isotropic hardening, the yield surface remains fixed in origin, orientation, and shape, but will change in size to accomodate plastic flow. Thus, if the initial yield function is written

$$f(\sigma) = g(\sigma) - \sigma_0 \tag{9.2}$$

the current yield function after plastic flow will be

$$f(\sigma, H) = g(\sigma) - \sigma_h \tag{9.3}$$

where σ_h is the largest value of $g(\sigma)$ attained during the preceding history.

In geometric terms, kinematic hardening states that the yield function remains fixed in orientation, shape, and size, but will change its origin to accomodate plastic flow. Thus

$$f(\underset{\sim}{\sigma}, H) = f(\underset{\sim}{\sigma} - \underset{\sim}{\varepsilon}^P/B) \qquad (9.4)$$

where $\underset{\sim}{\varepsilon}^P$ is the current plastic strain.

An alternative method for describing strain-hardening is the mechanical sublayer model proposed by White [26] and Besseling [27] and applied by Vaugh [28]. Each material element, infinitesimal or finite, is replaced by a number of subelements connected in parallel. If each sub-element is elastic/perfectly-plastic but with different yield stresses, the resulting total model has many similarities to kinematic hardening, except that the resulting B is piecewise constant rather than a single number. By including some subelements with isotropic hardening, models may be constructed which are intermediate to overall isotropic or kinematic hardening.

The subject of proper strain-hardening models is one of intense current interest. Indeed, an entire symposium was devoted to the topic at the 1976 ASME meeting and the interested reader is referred to the Proceedings of that meeting [29] for some of the current research being done in the area.

10. Circular plate. For a circular plate under rotationally symmetric loading, appropriate generalized stresses are the dimensionless moments

$$(m_r, m_\theta) = (1/M_0) \int_{-H}^{H} (\sigma_r, \sigma_\theta) z dz \qquad (10.1)$$

where $M_0 = \sigma_0 H^2$ is the yield moment and 2H the plate thickness. Since the principal directions are known and fixed, it is convenient to use Tresca's yield condition. Setting the third principal direction $\sigma_z = 0$ in (8.4) and using (10.1) we obtain

$$f = \max [|m_r|, |m_\theta|, |m_r - m_\theta|] - 1 \qquad (10.2)$$

as illustrated in Fig.* 21.

For a constant load the moments must satisfy the equilibrium equation

$$(rm_r)' - m_\theta = -3pr^2 \qquad (10.3)$$

Evidently if a rigid-plastic plate is plastic corresponding to one of the six sides of (10.2), the problem is statically determinate and easily solved. For example, the stress profile for a simply supported plate of unit radius lies everywhere on side BC

$$m_\theta = 1 \qquad (10.4a)$$

Substitution of (10.4a) in (10.3) and use of the boundary condition $m_r = m_\theta$ at $r = 0$ leads to

$$m_r = 1 - pr^2 \qquad (10.4b)$$

and the boundary condition $m_r(1) = 0$ furnishes the yield-point load

$$p = 1 \qquad (10.4c)$$

Before accepting (10.4) as the solution, two things must be verified. First, one must show that the stress profile lies on the finite side BC, which is more restrictive than the infinite line (10.4a). Since (10.4b,c) show that $0 \leq m_r \leq 1$ for all $0 \leq r \leq 1$, this condition is satisfied.

Second, we must associate a kinematically admissible velocity field with (10.4). Generalized strains for this problem

are

$$\dot{\kappa}_r = -\dot{w}'' \qquad \dot{\kappa}_\theta = -\dot{w}'/r \tag{10.5}$$

On side BC the strain-rate vector must be vertical and directed upwards. Thus

$$\dot{w}'' = 0 \qquad \dot{w}' = -C \qquad \dot{w} = C(1 - r) \tag{10.6}$$

where C is any positive constant.

At the center of the plate the slope jumps discontinuously from the symmetry value of 0 to the negative value -C. Thus, it follows from (10.5a) that $\dot{\kappa}_r$ is positively infinite. Since r = 0 is at the corner B in Fig. 21, a positive $\dot{\kappa}_r$ is admissible. Thus (10.6) is a kinematically admissible field and hence (10.4) is a complete moment solution.

A clamped plate is less simple, since the stress profile lies on BC near the center of the plate and on CD near the edge. The solution in this case is [3, Chap. 10]

$$0 \le r \le \eta: \quad m_\theta = 1 \qquad m_r = 1 - pr^2 \qquad \dot{w} = C\eta(1-\log \eta - r/\eta)$$

$$\eta \le r \le 1: \quad m_\theta = \log r + (3p/2)(1-r^2) \qquad m_r = m_\theta - 1 \tag{10.7a}$$

$$\dot{w} = -C\,\eta \log r$$

where p and η are defined by

$$3p - \log p - 5 = 0 \qquad p\eta^2 = 1 \tag{10.7b}$$

It is readily verified that the stress profile lies on the finite sides and that the velocity field is kinematically admissible.

As a final example of a rigid/perfectly-plastic plate we consider the annulus in Fig. 22 [30]. The stress profile in Fig. 23a is statically admissible, but the associated velocity

field shown in Fig. 23d is not kinematically admissible, since $\dot{\kappa}_\theta < 0$ for $1 < r < \xi$. The velocity profile in Fig. 23e would be kinematically admissible if associated with the stress profile in Fig. 23b, but it turns out that this profile is not statically admissible. The actual solution is shown in Fig. 23c,f, and involves an annulus of the plate remaining rigid. Details of this solution along with other rigid/perfectly-plastic plate problems may be found in [3, Chap. 10] and [31, Chap. 4].

We consider next an elastic/perfectly-plastic simply supported plate, using the idealized curve OED in Fig. 6. This is equivalent to considering an ideal sandwich plate. The general elastic solution for $\nu = 1/3$ is [32]

$$\begin{aligned} h^2\,\eta w' &= 4B/3r + 2Cr/3 + (p/3)r^3 \\ m_r &= B/r^2 - C - (5p/4)r^2 \\ m_\theta &= B/r^2 - C - (3p/4)r^2 \end{aligned} \tag{10.8}$$

where $h = H/A$, $\eta = E/\sigma_0$, and $w = W/H$.

For p sufficiently small the plate is everywhere elastic with

$$\begin{aligned} h^2\,\eta w' &= (p/6)(-5r + 2r^3) \\ m_r = (5p/4)(1 - r^2) \qquad & m_\theta = (p/4)(5-3r^2) \end{aligned} \tag{10.9}$$

This solution remains valid until $p = 0.8$ when the plate center reaches point B in Fig. 21. For p slightly larger than 0.8, the center of the plate will become plastic on side BC, with the outer annulus remaining elastic. Thus (10.4a,b) hold for $0 \le r \le \xi$ and (10.8) for $\xi \le r \le 1$. Using continuity at $r = \xi$ we obtain the complete moment solution

$$0 \le r \le \xi: \quad m_r = 1 + (p/4)(-\xi^4/r^2 + 2\xi^2 - 5r^2)$$

$$m_\theta = 1 + (p/4)(\xi^4/r^2 + 2\xi^2 - 3r^2) \qquad (10.10)$$

$$\xi \le r \le 1: \quad m_r = 1 - pr^2 \qquad m_\theta = 1$$

This solution holds until the entire profile lies on BC at the yield-point load $p = 1$.

To find the slope for $p > 0.8$, we observe that in the plastic regime BC, $\dot{\kappa}_r^p$ must vanish, so that

$$\eta H \dot{\kappa}_r = \eta H \dot{\kappa}_r^e = \dot{m}_r - \dot{m}_\theta/3 \qquad (10.11)$$

But (10.11) also held when the point in question was still elastic, so that it can be trivially integrated with respect to time to yield

$$h^2 \eta w'' = -(m_r - m_\theta/3) \qquad (10.12)$$

Therefore, the correct slope solution for $p > 0.8$ is

$$0 \le r \le \xi: \quad h^2 \eta w' = 2r/3 + (p/3)(-\xi^4/r - \xi^2 r + r^3)$$

$$\xi \le r \le 1 \quad h^2 \eta w' = 2r/3 + (p/3)(-2\xi^3 + r^3) \qquad (10.13)$$

The displacement, of course, can be found by integrating the slope with the boundary condition $w(1) = 0$. Curve (d) in Fig. 24 shows the resulting load vs. center deflection for the elastic/perfectly-plastic plate. Details of the solution may be found in [32].

This problem can also be solved for a elastic/strain-hardening material. The solution for $p < 0.8$ is, of course, the fully elastic one, independent of any potential strain-hardening. However, for $p > 0.8$, two plastic regions begin to form simultaneously at the plate center with $0 \le r \le \xi$ in the corner regime B, $\xi \le r \le \zeta$ on the side BC, and $\zeta \le r \le 1$

still elastic. For isotropic hardening the equations can be solved for each regime and the constants of integration determined by continuity and boundary conditions. For a value of p slightly greater than 1 (the exact amount will depend upon the strain-hardening constant), ζ will equal one. For larger p, the entire plate will be plastic with $0 \leq r \leq \xi$ in corner B and $\xi \leq r \leq 1$ on side BC. Algebraic details may be found in [32].

Figure 24 shows the load-deflection curves for both the elastic/strain-hardening and rigid/strain-hardening models. Aside from the fact that the "knee" in the curves which represents a partially plastic plate is curved rather than linear, Fig. 24 is qualitatively very similar to Fig. 4. Therefore, the same conclusions can be drawn from it, and we can gain confidence in our basic approach to plastic structures: namely that the rigid/perfectly-plastic model can be used to find the yield-point load, that strain-hardening can be neglected below the yield-point load, and that elastic strains can be ignored above it.

11. Finite element model. A finite element model has become the accepted way of solving complicated problems in elasticity, and usually the only question is which finite element model to use. Essentially, a trade off must be made between taking many simple elements with simple internal fields as opposed to fewer complex elements with complex fields.

Almost any finite element model for elasticity can be easily adapted to include plasticity with or without strain-hardening. However, there are certain features of plasticity which are basically different from elasticity and which may well affect the desirability of any given model.

Since plasticity must be formulated as a rate problem, the basic approach is as follows. At a generic time t_0, it is assumed that stress, strain, displacement, and any other quantities of interest are all known, and a finite element model is used to find the rates at time t_0. With all rates known, time is given a finite increment Δt and quantities at time $t_0 + \Delta t$ are approximated by

$$\phi(t_0 + \Delta t) = \phi(t_0) + \Delta t \, \dot{\phi} \, (t_0) \qquad (11.1)$$

The process is then repeated with t_0 replaced by $t_0 + \Delta t$.

There are, then, two distinct repeated stages to the solution: solving the rate problem and applying (11.1). We consider first three aspects of the rate problem. For definiteness we consider an elastic/perfectly-plastic material whose constitutive behavior is governed by Eqs. (8.6). The primary problem is involved with the branch points in (8.6f) and the inequalities (8.6a,b).

One of the simplest and most useful finite element models is the constant strain one which can be associated with arbitrary triangular or tetrahedral elements in two or three dimensions, respectively. With this element, f and $\dot{\lambda}$ will each have a constant value over the entire element, so that the decision concerning branch points must be made only on an element-by-element basis.

Now, at time t_0, f is known so that the first branch point in (8.6f) is no problem, and when $f < 0$ the element is elastic. However, $\dot{f}$ will be obtained as part of the rate solution so that it is not clear which branch should be used when $f = 0$.

A method which appears to work well in practice, at least for one-parameter loads, is to make any reasonable guess as to whether each element with $f = 0$ is elastic or plastic and solve the rate problem. Each element is then tested. If it was assumed elastic with $\dot{\lambda} = 0$, then $\dot{f}$ must be non-positive or else (8.6a) would be violated; if it was assumed plastic with $\dot{f} = 0$, then $\dot{\lambda}$ must be non-negative or else (8.6b) would be violated. Each element which fails its test has its assumption reversed and a new rate solution is found and tested. This process is continued until all elements simultaneously pass their test. A simple example has been constructed [11] in which all tests are not passed until the third iteration. Also, to the author's knowledge there is no proof that the iteration process will always converge, although there are no known counter examples. Further research is needed in this area, and meanwhile it is important that any finite element program continues to test all assumptions until a correct solution is obtained.

An alternative approach to the rate problem is to use the plastic minimum principles [33] and a numerical minimizing technique. The problem formulates as one in quadratic programming [34, 35]. The question of branch points is transformed to one of asking which constraints are active which is automatically handled by any quadratic programming program.

The second aspect of the rate problem lies in the choice of element. If any element has variable stress, then at time t_0 part of the element has $f < 0$ and part of it $f = 0$. For the $f = 0$ part, the branch-point questions raised above will exist with the further complication that the correct rate solution may be $\dot{f} = 0$ in part of that domain and $\dot{\lambda} = 0$ in the remainder. Even if this problem is solved, numerical integrations across the element will be necessary, thus substantially increasing the computer time spent in finding each rate solution. Therefore, questions concerning many simple versus few complex elements should be considered directly for elastic-plastic problems, with a strong presumption that simpler elements will be optimum than for purely elastic structures.

The final aspect of the rate problem is that of continuity. Elasticity problems are extremely continuous and efficient finite element methods will take advantage of that fact. However, problems for elastic/perfectly-plastic structures may have discontinuities in stress derivatives (as across the characterisitics in a plane strain problem) and even of stresses themselves as in Figs. 5d or 16. Stress discontinuities pose no particular problem, the finite element model merely forcing them to occur only at element boundaries, but velocity discontinuities may also occur. For example in Secs. 2 and 10 we saw that slope discontinuities could occur in beams and plates. It has been shown [36] that finite element models which allow for slope discontinuities are less efficient in the early stages of loading a beam, but become more efficient, i.e., give closer values for a given computation effort, as the yield-

point load is approached. A plate model in which slope discontinuities provide the only strains has been developed [37] and produced some valid results. Work is currently in progress [38] extending these ideas to problems in plane strain.

Even when the rate problem has been solved, there are questions to be answered concerning the application of Eq. (11.1). A plastic element requires $\dot{f} = 0$. Since the yield surface $f = 0$ is convex [23], if the stress point is not stationary, it must move along this convex surface. However, (11.1) is motion along a straight line tangent to the surface. Thus at time $t_0 + \Delta t$, the predicted f will be positive in violation of (8.6a).

A usual method of resolving this dilemma is to first use (11.1) to predict a new $\underset{\sim}{\sigma}$ which will, in general, have a positive f in each plastic element. We then replace $\underset{\sim}{\sigma}$ by $\beta\underset{\sim}{\sigma}$ where the scalar β is chosen so that $f(\beta\underset{\sim}{\sigma}) = 0$ in each plastic element. However, the stresses $\beta\underset{\sim}{\sigma}$ will not precisely satisfy the equilibrium equations so that some type of iteration must be performed.

If the yield function f is piecewise linear, then this problem disappears. The stress point may lie on one or more linear faces so that f and λ are replaced by f_i and λ_i throughout (8.6) and (8.6e) is replaced by

$$\dot{\underset{\sim}{\varepsilon}}^p = \Sigma\, \dot{\lambda}_i\, \nabla f_i \qquad (11.2)$$

If the external loading is linear, Eq. (11.1) will now be exact until either an elastic element becomes plastic or until a plastic element encounters a new face.

The yield function is, of course, a physical property of the material. However, it can only be measured with limited

accuracy, so that it is reasonable to approximate it by any convenient function. For finite element models, a piecewise linear approximation has the obvious advantage of eliminating the problem associated with (11.1) and any strictly convex yield function. A systematic procedure for constructing a piecewise linear approximation to a given nonlinear f is given in [39].

A third possible solution to this difficulty is to introduce a small plastic viscosity [40, 41]. The resulting visco-plastic model permits expansion of the yield surface, but for small ν the expansion would be severely limited so that the solution will be very close to that for a perfectly-plastic material. Indeed, for some real materials the visco-plastic model may be more realistic than the perfectly-plastic one.

The preceding discussion of (11.1) has been implicitly based upon a model with constant stress in each element. For a more complex element, the problem would be equally present, and all of the suggested remedies would be more difficult to apply. For this stage too, then, there are strong arguments in favor of using a large number of simple elements in the solution of plasticity problems.

12. Conclusions. It is evident that the preceding sections make no claim to completeness either in content or in references. We have tried merely to sample the vast field of plastic structures, beginning with the simplest truss and beam problems in the hope of rousing the reader's interest. Many interesting and important topics have had to be omitted entirely. Among these

omissions are plastic buckling, effect of geometric changes, and dynamic effects, and we have not even mentioned the vast literature on plastic shells [42].

The reader interested in more details concerning the material covered will find most of it and more in [3]. For the material not covered, almost every new issue of most mechanics journals contains articles extending the theory of plasticity and the list of problems which it has solved.

REFERENCES

1. D. Vasarhelyi and R. A. Hechtman: Welded reinforcement of openings in structural steel members, Welding J. Research, Suppl., 31, 169s-180s (1952).

2. J. Marin: Stress-strain relations in the plastic range for biaxial stresses, J. Franklin Inst., 248, 231-249 (1949).

3. Philip G. Hodge, Jr.: "Plastic Analysis of Structures", McGraw-Hill Book Co., Inc., New York, 1959.

4. A. A. Gvozdev: The determination of the value of the collapse load for statically indeterminate systems undergoing plastic deformation, "Proceedings of the Conference on Plastic Deformations," Akademiia Nauk SSSR, Moscow-Leningrad, 1938, pp. 19-33; translation into English by R. M. Haythornthwaite, Int. J. Mech. Sci. 1, 322-335 (1960).

5. R. Hill: On the state of stress in a plastic-rigid body at the yield point, Phil. Mag. 42 (7), 868-875 (1951).

6. R. Hill: A note on estimating the yield-point loads in a plastic-rigid body, Phil. Mag. 43 (7), 353-355 (1952).

7. H. J. Greenberg and W. Prager: Limit design of beams and franes, Proc. ASCE 77 (Sep. 59), 1951.

8. D. C. Drucker, H. J. Greenberg, and W. Prager: The safety factor of an elastic-plastic body in plane strain, J. Appl. Mech. 18, 371-378 (1951).

9. D. C. Drucker, W. Prager, and H. J. Greenberg: Extended limit design theorems for continuous media, Q. Appl. Math. 9, 381-389 (1952).

10. D. C. Drucker: Plasticity of metals-mathematical theory and structural applications, Trans. ASCE, 116, 1059-1072 (1959).

11. P. G. Hodge, Jr.: Complete solutions for elastic-plastic trusses, SIAM J. Appl. Math. 25, 435-447 (1973).

12. F. Stüssi and C. F. Kollbrunner: Beitrag zum Traglastverfahren, Bautechnik, 13, 264-267 (1935).

13. W. Prager: The general theory of limit design, Proc. 8th Intern. Congr. Appl. Mech., Istanbul, 1952, 2, 65-72 (1956).

14. William Prager and Philip G. Hodge, Jr.: "Theory of Perfectly Plastic Solids," Univ. Microfilms Internat. Ann Arbor, Mich ("Books on Demand" OP69234), orig. J. Wiley and Sons Inc., New York, 1948.

15. H. Tresca: Mémoire sur l'écoulement des corps solides, Mém. pres. par div. sav. 18, 733-799 (1868).

16. R. v. Mises: Mechanik der festen Koerper im plastisch deformablen Zustand, Goettinger Nachr., math.-phys. Kl. 1913, 582-592 (1913).

17. B. de Saint Venant: Mémoire sur l'établissement des équations différentielles des mouvements intérieurs opérés dans les corps solides ductiles au delà des limites ou l elasticite pourrait les ramener a luer premier etat, C. R. Ac. Sci. (Paris) 70, 473-480 (1870).

18. M. Lévy: Mémoire sur les équations générales des mouvements intérieurs des corps solides ductiles au delà des limites où l'élasticité pourrait les ramener à leur premier état, C. R. Ac. Sci (Paris) 70, 1323-1325 (1870).

19. L. Prandtl: Spannungsverteilung in plastischen Koerpern, Proc. 1st Internat. Congr. Appl. Mech. (Delft, 1924), pp. 43-54.

20. E. Reuss: Beruecksichtigung der elastischen Formaenderungen in der Plastizitaetstheorie, Z. angew. Math. Mech. 10, 266-274 (1930).

21. R. v. Mises: Mechanik der plastischen Formaenderung von Kristallen, Z. angew. Math. Mech., 8, 161-185 (1928).

22. R. Hill: Plastic distortion of non-uniform sheets, Phil. Mag. (7), 40, 971-983 (1949).

23. D. C. Drucker: Some implications of work hardening and ideal plasticity, Q. Appl. Math. 7, 411-418 (1950).

24. W. Prager: A new method of analyzing stresses and strains in work-hardening plastic solids, J. Appl. Mech. Trans. ASME, 78, 493-496 (1956).

25. W. Prager: The theory of plasticity--A survey of recent achievements, Proc. Inst. of Mech. Eng., 169, 41-67 (1955).

26. G. N. White, Jr., Application of the theory of perfectly plastic solids to stress analysis of strain hardening solids", GDAM Rep. 51, Brown University, 1950.

27. J. F. Besseling, A theory of plastic flow for anisotropic hardening of an initially isotropic material, Rep. S410, Nat. Aero. Res. Inst., Amsterdam, 1953.

28. D. K. Vaughan, A comparison of current work-hardening models used in the analysis of plastic deformations, Ms. Thesis, Texas A & M University, 1973.

29. "Constitutive Equations in Viscoplasticity-Computational and Engineering Aspects, J. Stricklin and K. J. Saczalaski, eds., American Society of Mechanical Engineers (Winter Annual Meeting), New York, 1976.

30. P. G. Hodge, Jr.: Yield point load of an annular plate, J. Appl. Mech. 26, 454-455 (1959).

31. Philip G. Hodge, Jr.: "Limit Analysis of Rotationally Symmetric Plates and Shells," Univ. Microfilms Internat., Ann Arbor, Mich. ("Books on Demand OP63418), orign. Prentice-Hall, Inc., Englewood Cliffs NJ, 1963.

32. P. G. Hodge, Jr.: Boundary value problems in plasticity, "Plasticity", E. H. Lee and P. S. Symands, eds., Pergammon Press, New York, 1960, pp. 297-337.

33. H. J. Greenberg: Complementary minimum principles for and elastic-plastic material, Q. Appl. Math. 7, 85-95 (1949).

34. P. G. Hodge, Jr., T. Belytschko, and C. T. Herakovich: Quadratic programming and plasticity, "Computation Approaches in Applied Mechanics," E. Sevin, Ed., American Society of Mechanical Engineers, New York, 1969, pp. 73-84.

35. P. G. Hodge, Jr., V. K. Garg, and S. C. Anand: A finite element method for plasticity problems, "Developments in Theoretical and Applied Mechanics" Vol. 7, M. Chi, Ed., Catholic University, Washington, 1974, pp. 369-383.

36. P. G. Hodge, Jr.: Finite element methods in plasticity, "Proc. 7th U.S. Nat. Congr. Appl. Mech.", S. K. Datta, ed., Amer. Soc. Mech. Engs., New York, 1974, pp. 114-119.

37. P. G. Hodge, Jr. and A. A. McMahon: A simple finite element model for elastic-plastic plate bending, Comp & Struct 2, 841-854 (1972).

38. H. v. Rij: Ph.D. dissertation, Univ. of Minn (in preparation).

39. P. G. Hodge, Jr.: Automatic piecewise linearization in ideal plasticity, Comp. Methods in Appl. Mech. and Eng., 10, 249-272 (1977).

40. Q. S. Nguyen and J. Zarka: Quelques méthodes de résolution numérique en elastoplasticité classique et en elasto-viscoplasticité, Séminaire Plasticité et Viscoplasticité 1972, Ecole Polytechnique, Paris; see also Discussion of [36].

41. O. C. Zienkiewicz: Discussion of [36].

42. P. G. Hodge, Jr.: Plastic analysis and pressure vessel safety, Appl. Mech Rev. 24, 741-747 (1971).

(a)

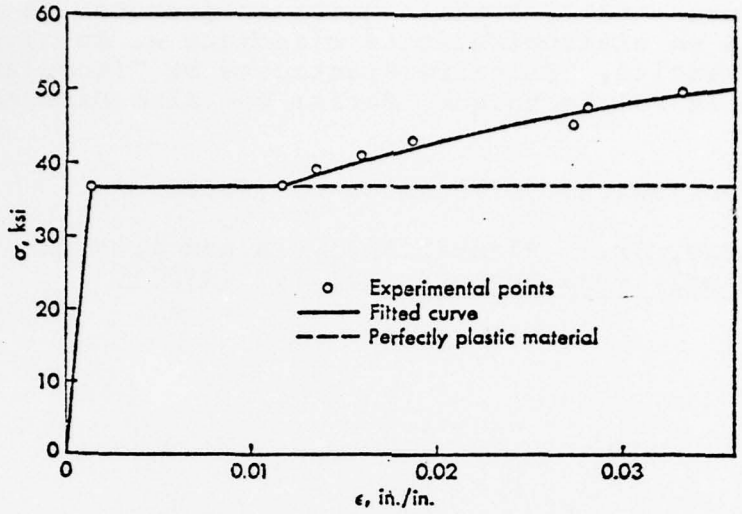

(b)

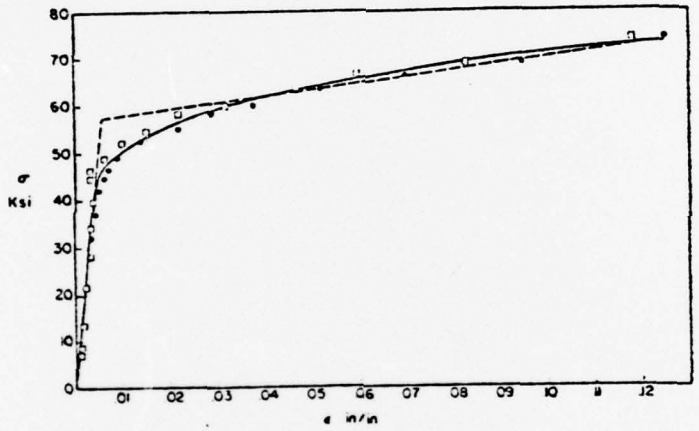

Fig. 1. Stress-strain curves

a. Mild steel

b. 24 S-7 aluminum

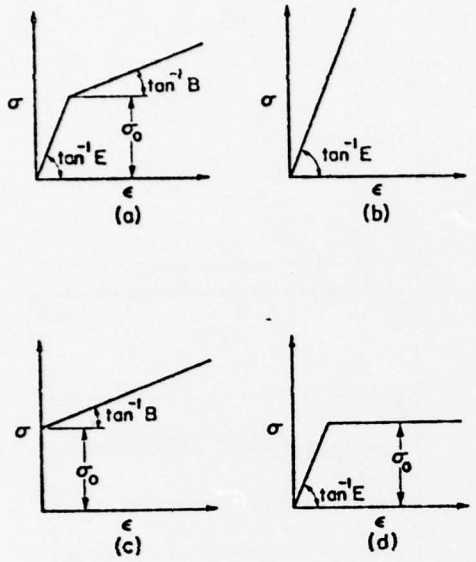

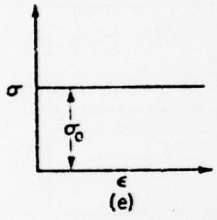

(a) Elastic/strain hardening
(b) Elastic
(c) Rigid/strain hardening
(d) Elastic/perfectly plastic
(e) Rigid/perfectly plastic

Fig. 2—Ideal stress–strain curves

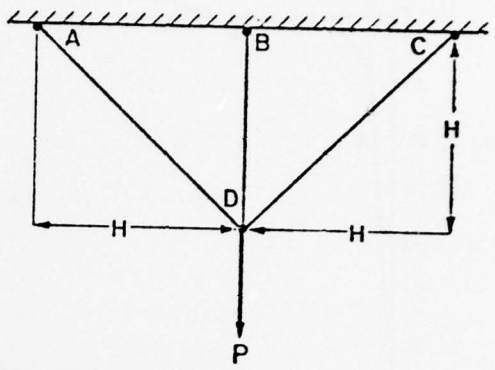

Fig. 3—Three-bar truss

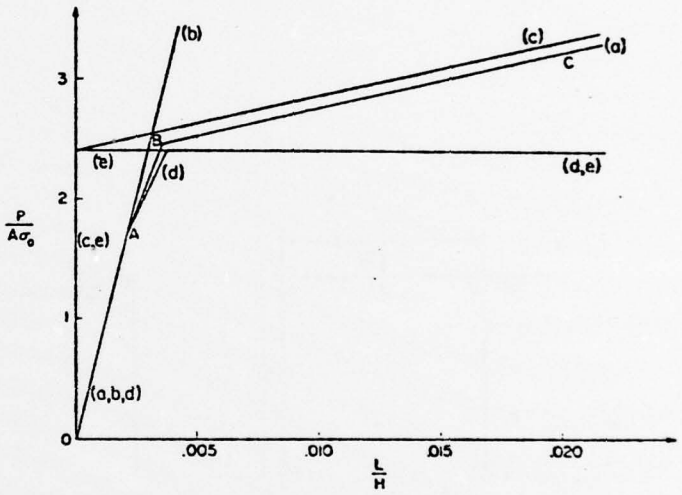

Fig. 4—Load-displacement curves for truss (letters in parentheses refer to the materials of Fig. 2)

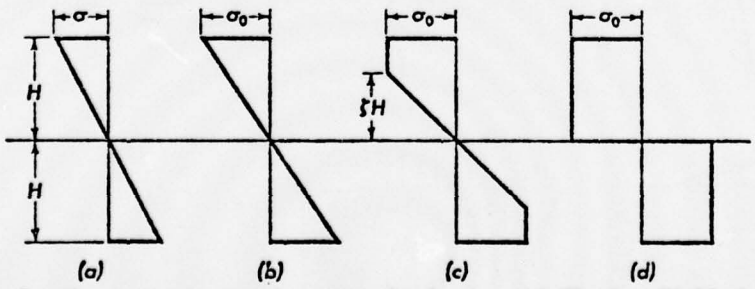

FIG. 5 Stress distributions in rectangular beams. (*a*) Elastic. (*b*) Maximum elastic, $M = M_e$. (*c*) Elastic plastic. (*d*) Maximum plastic, $M = M_0$.

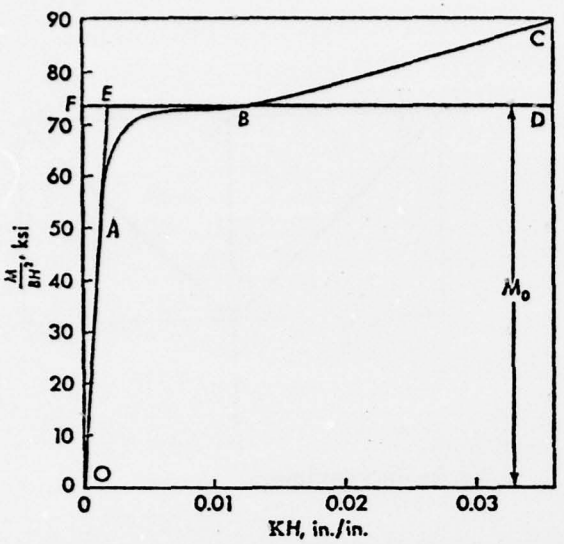

FIG. 6. Moment curvature relations. *OABD*, perfectly plastic material. *OABC*, mild steel. *OAED*, ideal section. *OFED*, rigid plastic material.

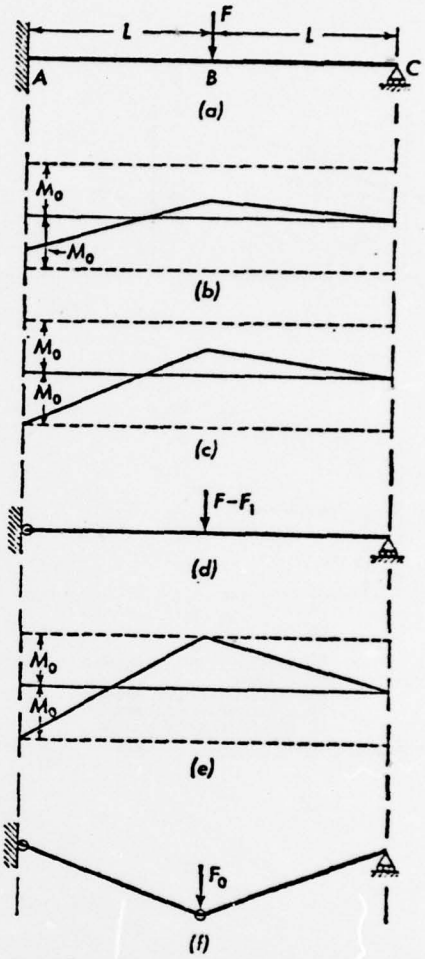

FIG. 7 Collapse of singly indeterminate beam. (*a*) Loaded beam. (*b*) Elastic moments. (*c*) One-hinge moment distribution. (*d*) Beam with one hinge. (*e*) Collapse moments. (*f*) Collapse mechanism.

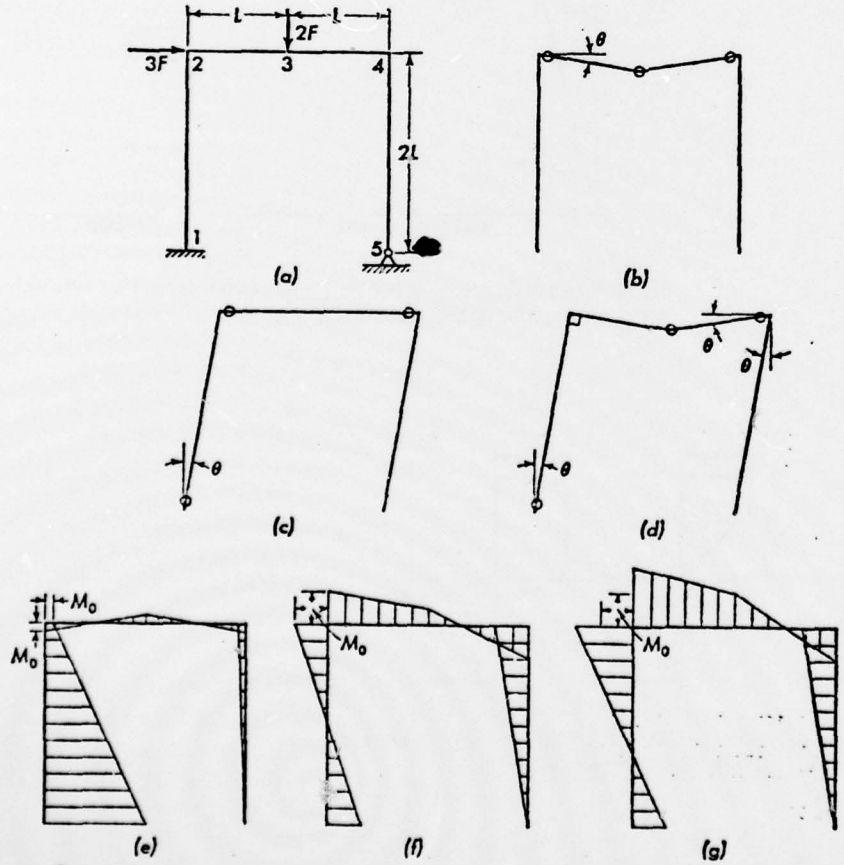

FIG. 8 Collapse of simple frame. (*a*) Loaded frame. (*b*) Collapse mode for beam failure only. (*c*) Collapse mode for panel failure only. (*d*) Combined collapse mode. (*e*) Moment distribution for (*b*) (not admissible). (*f*) Moment distribution for (*c*) (statically admissible). (*g*) Moment distribution for (*d*) (not admissible).

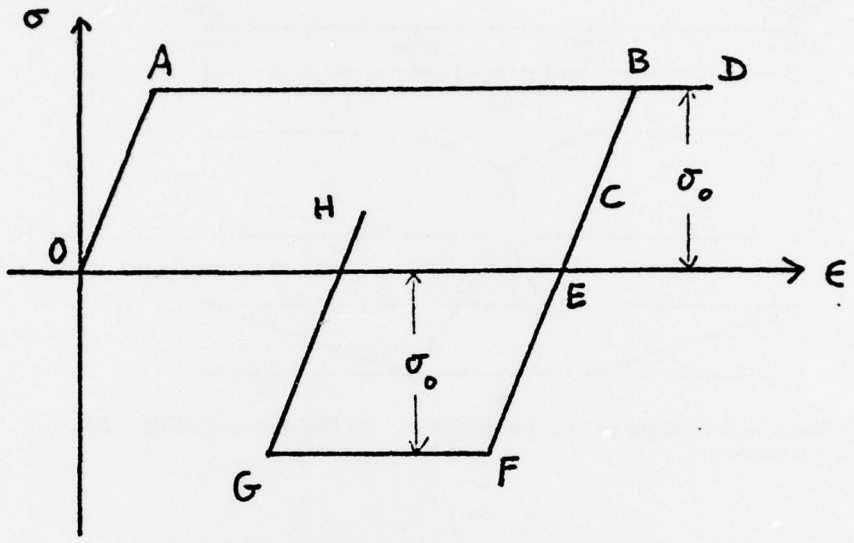

Fig. 9 Unloading and reloading of perfectly-plastic material

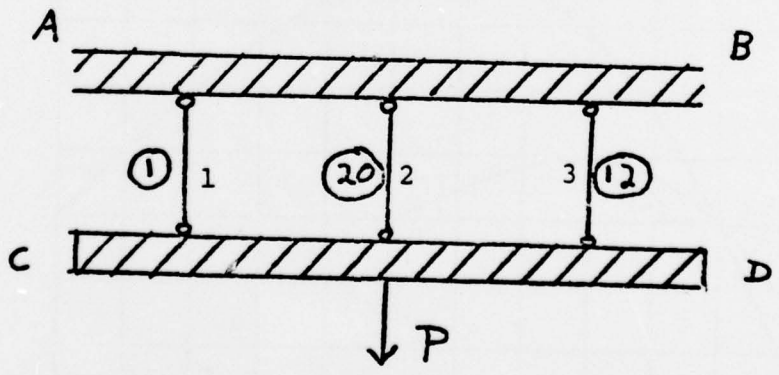

Fig. 10 Three-bar truss

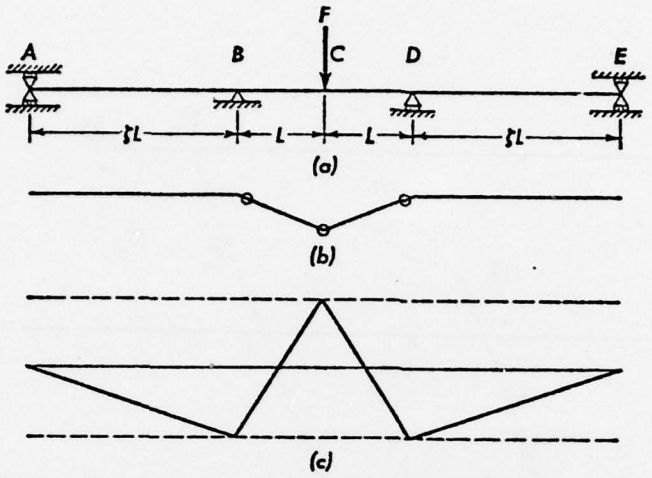

FIG. 11 Beam on four supports. (*a*) Loaded beam. (*b*) Collapse mechanism. (*c*) Moment distribution.

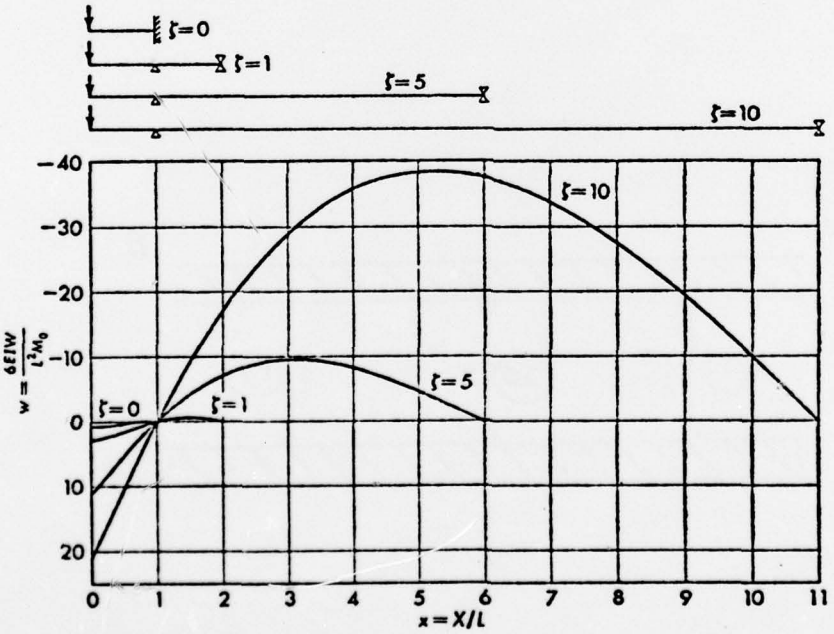

FIG. 12 Deformed shape at collapse of beam on four supports.

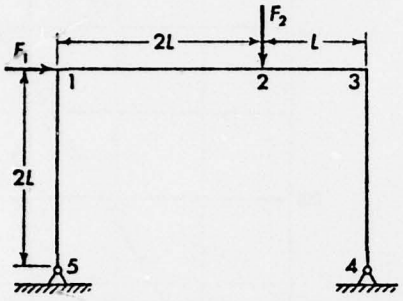

FIG. 13 Frame under two time-dependent loads.

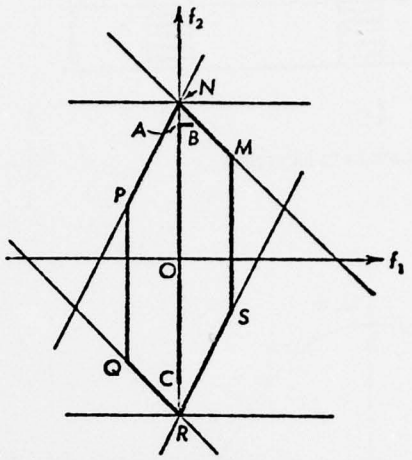

FIG. 14 Domain of admissible loads for frame of Fig. 13

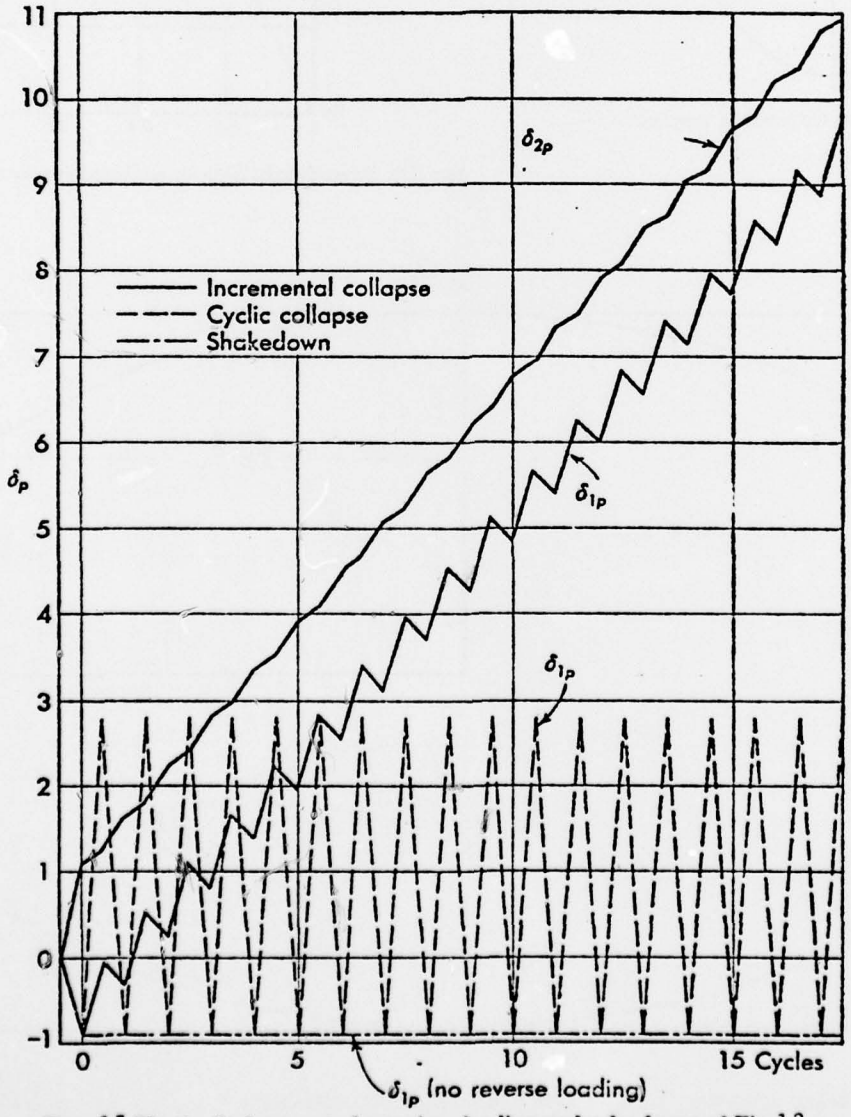

FIG. 15 Plastic displacements for various loading cycles for frame of Fig. 13

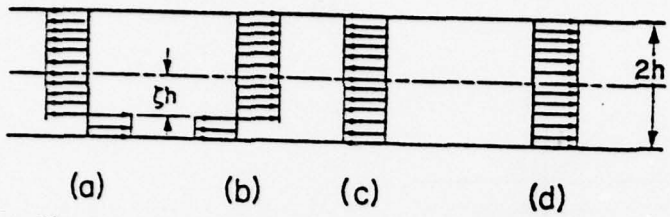

Fig. 16 -Stress distributions for beam in tension and bending

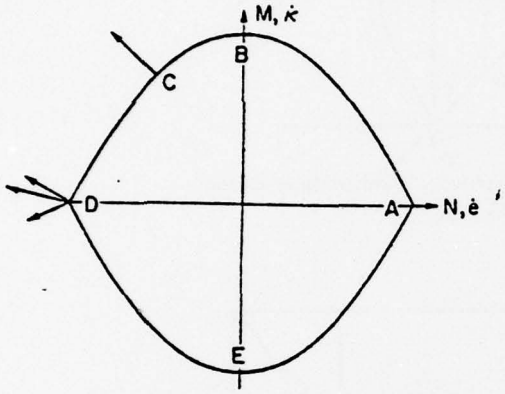

Fig. 17-Interaction curve for beam in tension and bending

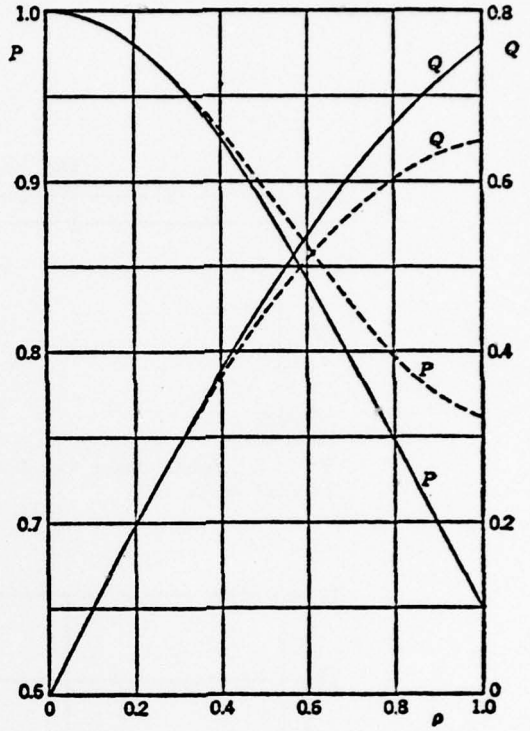

FIG. 19 Stress distributions for combined tension and torsion of circular cylinder

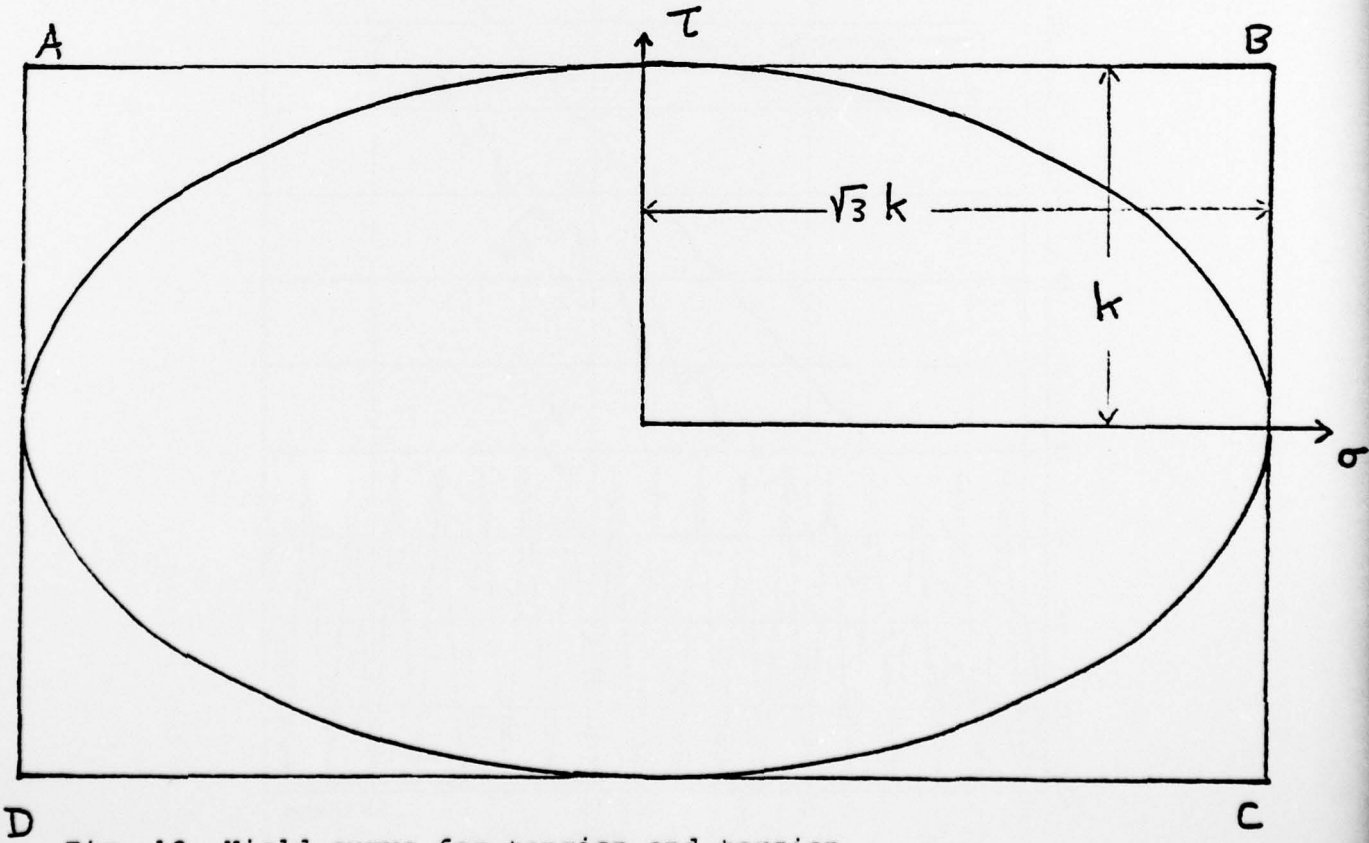

Fig. 18 Yield curve for tension and torsion

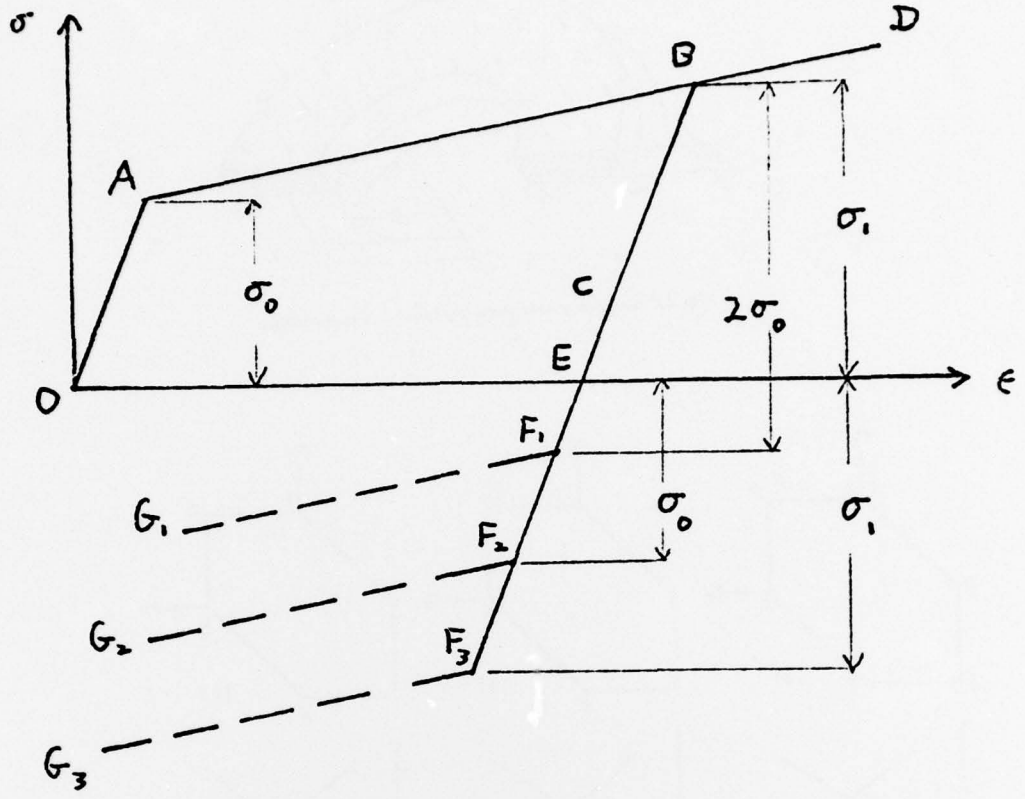

Fig. 20 Unloading and reloading of strain-hardening material

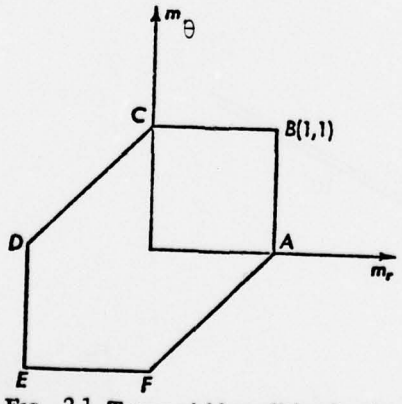

FIG. 21 Tresca yield condition for circular plates.

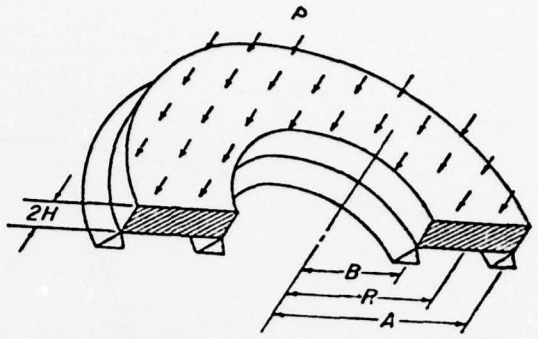

Fig. 22 Annular plate, showing load and dimensions

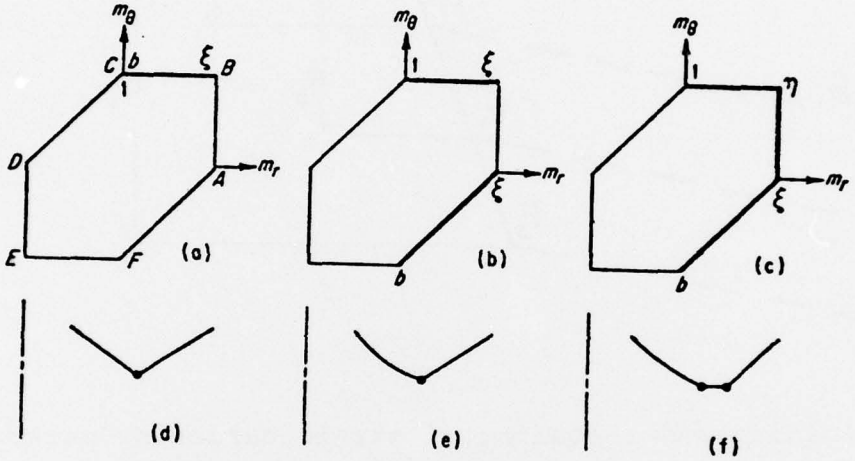

Fig. 23 Stress and velocity profiles for annular plate: (a) statically admissible stress profile; (b) statically inadmissible stress profile; (c) correct stress profile; (d) kinematically inadmissible velocity profile; (e) kinematically admissible velocity profile; (f) correct velocity profile

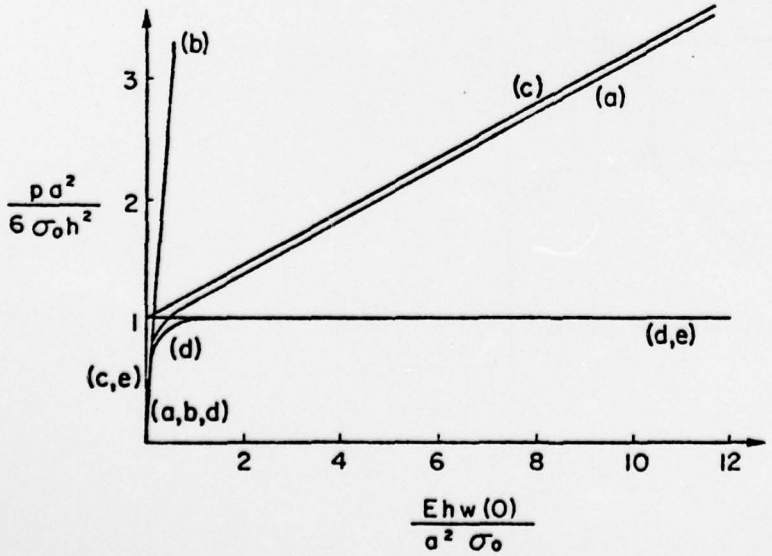

Fig. 24—Load–displacement curve for circular plate (letters in parentheses refer to the materials of Fig. 2)